Examining the molecular consequences of disrupted clock-gene expression in the mouse striatum

Idi (Jeremie) Shabani

A Thesis

in

The Department

of

Biology

Presented in Partial Fulfillment of the Requirements

for the Degree of Masters of Science (Biology) at

Concordia University

Montreal, Quebec, Canada

February 2022

CONCORDIA UNIVERSITY
School of Graduate Studies

This is to certify that the thesis prepared

By: Idi (Jeremie) Shabani

Entitled: Examining the molecular consequences of disrupted clock-gene expression in the mouse striatum

Submitted in partial fulfillment of the requirements for the degree of

Master of Science (Biology)

Complies with the regulations of the University and meets the accepted standards with respect to originality and quality.

Signed by the final Examining Committee:

Dr. Paul Joyce_____ Chair & Examiner

Dr. Shimon Amir _____ Thesis Supervisor

Dr. Michael Hallett_____ _____Examiner

Dr. Vladimir Titorenko _____External Examiner

Approved by Dr. Grant Brown_____ Graduate Program Director

Dr. Pascale Sicotte_____Dean of Faculty

Date: March 30, 2023

ABSTRACT

Examining the molecular consequences of disrupted clock-gene expression in the mouse striatum

Idi (Jeremie) Shabani

Most organisms possess biological pacemakers that generate daily oscillations ranging from molecular processes to rhythms in physiology and behavior. In mammals, this system is composed of a master clock, located in the Suprachiasmatic Nucleus (SCN), and several peripheral clocks found in various tissues and brain regions. Previously, it has been identified that genome-wide or tissue-specific disruptions of circadian clock-genes such as *Bmal1* are associated with mood disorders. Particularly in the striatum, a brain region that is vital in the motor and reward systems. Interestingly, the exact underlying molecular mechanisms are not well understood. In this study, gene expression of the receptors corresponding to GABAergic, Dopaminergic and Glutamatergic signalling in the dorsal striatum of adult Male and Female mice with a conditional knockout of *Bmal1* (ie: KO – knockout vs. WT- Wild Type) were evaluated at two different time points (ZT2 and ZT14) in order to determine the effect of a clock manipulation on the expression of *DRD2*, *MAOA*, *A2a*, *GABBR1,* and *GAD67*. The gene expression of these candidate targets was studied to gain a deeper understanding of the mechanism through which Bmal1 is linked to mood disorders and elucidate a clearer role on the influence of clock-controlled genes with relation to GABAergic, Glutamatergic, and Dopaminergic receptors. Evidence has suggested that disrupted clock function dysregulates cell signalling which contributes to the development of behavioral phenotypes associated with mood disorders. However, the etiology remains unclear. Therefore, this experiment allowed us to further examine the underlying molecular pathways associated with behavioral phenotypes observed in striatal-dependent clock gene knockout mice. Results indicated no significant differences in gene expression were observed in the candidates following gene deletion. Interestingly, different mis-regulation trends were observed in the targets, suggesting *Bmal1* may play a role in the dysregulation of the candidates selected.

ACKNOWLEDGEMENTS

First and foremost, I would like to acknowledge my supervisor Dr. Shimon for giving me the opportunity to complete my masters project in his laboratory. Your support and expertise has allowed me to investigate the interdisciplinary aspects of molecular genetics and behavioral neuroscience. Furthermore, I would like to thank Dr. Konrad Schottner for his mentorship throughout the formulation and execution of this thesis project. His guidance was vital and he answered all my questions with appropriate feedback which I am truly thankful for. Special thanks to Cassandra Goldford who provided support in generating the knockout mice used in this thesis project. I would also like to thank Nuria de Zavalia for her assistance and valuable feedback throughout the writing process. Thank you to my committee members, Dr. Michael Hallett, Dr. Vladimir Titorenko and Dr. Paul Joyce, for taking the time to review my thesis and provide me with suggestions to improve the quality of the present study. Finally, I would like to thank all other members of the AMIR LAB, NSERC, CIHR, and FRQS for their assistance throughout the preparation and funding of this thesis project.

Table of contents

List of Figures

List of Tables

INTRODUCTION

Circadian rhythms (CRs) are internal clocks that generate daily oscillations. These rhythms are essential in ensuring that the body's processes are optimized at various points during a 24-hour period (Vetter, 2018). Mammals have a circadian system composed of a master clock and several peripheral clocks in various tissue and brain regions. The master circadian pacemaker is located in the suprachiasmatic nucleus (SCN) of the hypothalamus and coordinates rhythmic output of peripheral clocks and aligns them to external time (Ketchesin & McClung, 2018). Different pathways synchronize peripheral clocks to the light-dark (LD) cycle with light being the most important zeitgeber for circadian clocks. Zeitgebers are rhythmic signal(s) capable of entraining circadian clocks and can be external (ie: outside temperature) or internal (ie: social interactions; Bordyugov et al., 2018; Falcon et al., 2013). The coordination of these self-sustained oscillations with external time is known as entrainment. The process of entrainment provides a stable phase relationship between the oscillator and the zeitgeber. Abnormal light exposure can desynchronize the circadian rhythms of an organism by disrupting the function of the master SCN clock. Disturbances of the clocks are expressed in different manners and contribute to changes in sleep–wake cycles, blood pressure, hormone secretion, and behaviour (Ikeda et al., 2018; Kervezee et al., 2018). In humans, these changes are observed in many ways such as in shiftwork or during jet lag (crossing multiple time zones in a short period of time which can cause one to struggle to acclimatize to the changes in L/D cycle). There has been considerable progress concerning the role of clock disturbances on health, but further studies employing different approaches are warranted to understand the mechanism between such disturbances and the mammalian clock.

At the molecular level, circadian clockwork generates daily oscillations of clock gene expression via a transcriptional/ translational feedback loop (TFFL), which is widely conserved across species (Bordyugov et al., 2018). In this cellular model the transcription of clock genes are regulated by their own protein product (Varinthra & Liu., 2019). In mammals, the molecular clock is composed of both a positive (1 – BMAL: CLOCK dimer) and negative (2- PER:CRY complexes) component. Essentially, the transcription factors BMAL1/ and CLOCK form a complex which drives the transcription of Period and Cryptochrome genes via interactions with E-box promoter elements, a key event in the regulation of clock and clock-controlled gene expression. (McClung, 2019; Figure 1). Previous bioinformatics analyses identified E-boxes and E1-E2 sites as BMAL1/CLOCK consensus sites in vertebrates, both of which influence transcriptional activity in luciferase reporter assays, an assessment that examines whether a protein can activate/repress the expression of a target gene using a reporter protein (Munoz et al., 2006; Carter & Shieh, 2015). Therefore, the binding of BMAL1/CLOCK to E1-E2 elements involves a cooperative and spacing-dependent interaction between the tandem sites (Rey et al., 2011). From a genomic perspective, this suggests that E-boxes recruit BMAL1/CLOCK heterodimers rhythmically, while E1-E2 elements influence the core clock elements to ensure accuracy in timing of the circadian clock.

This is important because in turn, PER and CRY proteins form complexes which migrate to the nucleus and inhibit the action of the BMAL:CLOCK ultimately inhibiting Per and Cry transcription(Varinthra & Liu., 2019; McClung, 2019). Finally, phosphorylation controls the dynamics of Per nuclear entry, stability and ubiquitination. This permits the controlled degradation of the PER:CRY complex and the BMAL:CLOCK dimer becomes active again allowing the 24-h feedback loop to restart (Figure 1). Several advancements have been made in understanding how the positive and negative transcriptional regulators interact at a molecular level over the circadian cycle and affect circadian timing.

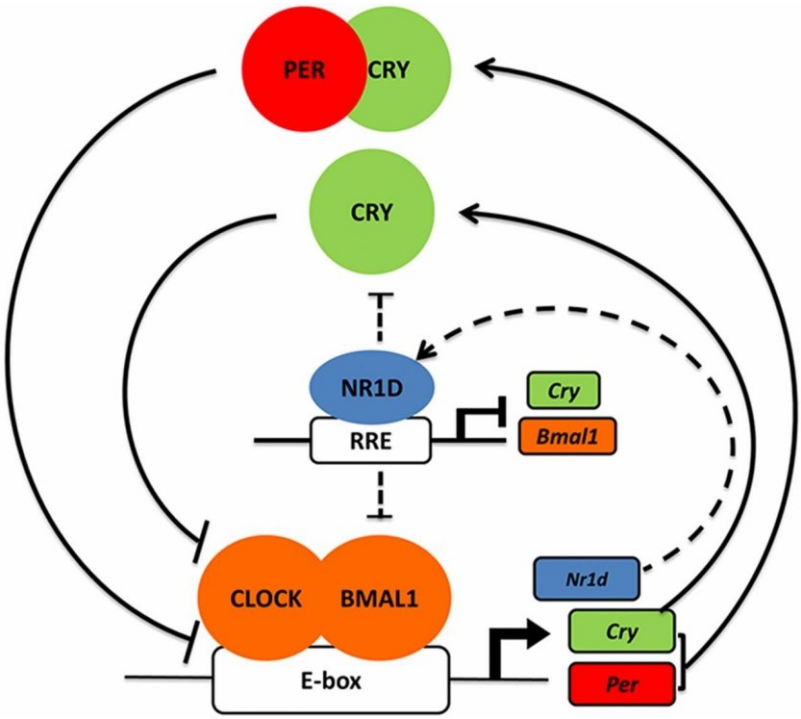

Figure 1: TTFL model for the mammalian circadian clock (Chiou et al., 2016). Protein dimers of the Brain and muscle arnt-like 1 (Bmal1) and Circadian locomotor output cycles kaput (Clock) genes form the positive arm of the loop by activating transcription of Period (Per) and Cryptochrome (Cry) genes and interfering with transactivation, and PER by causing the displacement of CLOCK–BMAL1 from E-boxes in a CRY-dependent manner (Schoettner et al., 2022). By their inhibitory interaction with BMAL1/CLOCK, dimerized PER/CRY proteins repress their own transcription, thus forming the negative arm of the loop that repeats every 24 h (Takahashi, 2017). Degradation of PER and CRY ceases their repressing function so that the cycle of transcription/translation can start again. The secondary loop regulates transcriptional activity of Bmal1 through Retinoid orphan receptor (ROR-a, b, g) and Rev-Erb-a/b. Rhythmic output of the clock is generated by the expression of clock-controlled genes (CCGs) which influence the regulation of vital cellular functions like metabolism and cell signaling (Bozek et al., 2009; Schoettner et al., 2022).

The striatum has recently been found to be a region of interest in the study of circadian disturbances (CD). Evidence from both human and animal studies support the relation between the circadian system and striatum-related behaviours. Previous literature indicates that impairment of the striatum, specifically, global and striatal-specific ablation of various clock genes expression such as *CLOCK* and *Nrd1*in mice are associated with the behaviors seen in mood disorders and substance abuse problems (Schnell et al., 2015; Landgraf et al., 2016). Furthermore, global disruptions of *Bmal1*, a gene of interest in this study, is strongly associated with CDs which contribute to the development of neuropsychiatric disorders, and premature aging (Ripperger & Schibler, 2006). Thus, disruption to the striatal clock has been suggested to contribute to the development of mood disorders and must be further investigated to elucidate how CDs impair the neural functioning of medium spiny neurons (MSN), an early pathological marker of many mood disorders (Harbour et al., 2014). The striatum is located in the basal ganglia and is composed of three different cell types: Cholinergic interneurons, Medium Spiny Neurons (MSN), and GABAergic interneurons which are subdivided into two regions: ventral striatum (VS) and dorsal striatum (DS) that regulate mood arousal and central executive functioning (McClung 2019; Harbour et al., 2014). The MSN's comprise approximately 95% of striatal neurons and have two primary phenotypes namely D1-type (direct pathway) and D2-type (indirect pathway).They receive synaptic inputs from

glutamatergic and dopaminergic afferents of the basal ganglia circuitry to influence behavioral output (Albrecht, 2012). Dopamine is a neurotransmitter which plays a modulatory role in of reward, motivation and addiction. This chemical messenger works in tandem with the glutamate neuronal system to create a balance of neurotransmission in these regions (Mendoza & Challet 2014). The dysregulation of this interaction has been associated with (CD) and may contribute to the development of neuropsychiatric illnesses (Kim et al., 2017; McClung, 2013; Marchard & Yurglelunn-Todd, 2010)

Presently, the etiology of several psychiatric disorders is not well understood. They can have a debilitating effect on the daily lives of those affected, and evidence has revealed that approximately 1 in 3 Canadians will be affected by a mental illness in their lifetime (Health Canada 2020). Growing evidence suggests the comorbidity of circadian clock gene disturbances in various mood disorders. Previous literature has demonstrated that striatal specific alterations of clock genes to be the cause for these conditions, perhaps by the interaction with the dopamine signaling pathway (Kim et al., 2017). However, there has also been growing interest in the implications of abnormal glutamatergic, and GABAergic neurotransmission (Kumar 2019; Chi-Castena & Ortega, 2018). Generally, neurons are activated by glutamate (most abundant excitatory neurotransmitter in the adult central nervous system of mammals), and depressed by GABA, a major inhibitory neurotransmitter in the mammalian brain and the principal neuron in the striatum (Zhang & Qu, 2018). Evidence has suggested that alterations in the activation of these systems modulates circadian rhythms in the brain highlighting their role in the pathophysiological basis of neurological disorders (Ono et al., 2020; Perez et al., 2003; Zhang & Qu, 2018).

Additionally, clock gene expression within the striatum is sensitive to dopamine release (Hood et al., 2010). This evidence suggests circadian clock gene expression and dopamine signaling mutually influence each other to potentially regulate psychiatric disorders. Supporting this notion, the two main groups of glutamate (metabotropic and ionotropic – AMPAR, NMDAR, KAR) and dopaminergic receptors (D1, D2) are strongly implicated in the etiology of many mood disorders. The metabotropic group interacts with G-proteins and is classified into three main groups based upon sequence homology (Korshunov et al., 2017). The ionotropic group are expressed in the areas of neuronal circuits involved in mood regulation. GABAergic signalling is subdivided into two groups namely GABAA (ionotropic) and GABAB (mainly expressed in dorsal area; metabotropic) with both playing a role in the development of mood disorders (Ono et al., 2018). This evidence suggests that clock malfunctions may influence the functional role of these receptors, but the mechanism of action employed remains relatively unknown. Therefore, it is imperative that we further examined these candidates to determine whether clock gene expression may be influenced by different signalling pathways.

Preliminary results strongly indicate that targeted Bmal1 deletion from MSNs is associated with mood disorders, albeit in sex-specific fashion (de Zavalia et al., 2020). On the basis of this preliminary evidence, we sought to further investigate whether the disruption of Bmal1 gene activity in the striatum would affect the expression of candidate targets. Precisely, this thesis evaluated the effect of a clock manipulation on the expression of Glutamate, Dopaminergic and GABA receptors. This was accomplished by determining the expression of candidate genes using qPCR. Specifically, I compared the expression of genes encoding glutamatergic receptors, genes encoding GABAergic receptors, along with genes encoding dopamine receptors in the striatum of *Bmal1* striatal-knockout (SKO) and wild-type (WT) controls. Using this method, we hypothesized that deletion of *Bmal1* in striatal MSNs will affect the gene expression of Glutamatergic, Dopaminergic, and GABAergic receptors.

MATERIALS & METHODS

Design Rationale. The experiment involved 12 to 20-week-old male and female transgenic mice bearing floxed alleles of the *Bmal1* gene. The design consisted of a total of 3-4 mice/group (1- Wild type, 2- Striatal Knockout) tested at 2 different time points (ZT2 – 2 hours before lights on, and ZT14 – 2 hours before lights off). The use of Cre-lox technology was employed to generate a striatal *Bmal1* knockout line. This method permits site specific recombination events in genomic DNA using an enzyme known as "Cre"(Lanza, Dyess & Alper, 2012). This component recognizes and targets the specific sequence of interest (LoxP). Competent mice were kindly provided by Konrad Schottner.

Sample Collection & RNA Preparation. Mice were sacrificed, and the brains were collected, flash frozen in isopentane, and subsequently stored at -80C. Following collection, serial coronal sections (100 µm thick of the dorsal striatum) were obtained from the brain using a standard Cryostat. Tissue punches from the dorsal striatum (1.5mm in diameter) in accordance with the mouse brain atlas (Paxinos and Franklin, 2004) were kindly collected by Cassandra Goldfarb from naïve animals and stored at -80C and later used for RNA extraction.

Total RNA was extracted using a phenol/chloroform extraction method under specific conditions (Table 1; Invitrogen Trizol Reageant)[31]. The quantity and quality of the RNA was assessed with spectrophotometry and the RNA integrity test. A ratio of 1.8-2.0 is indicative of a pure RNA sample, while a value below or above that range for the 260/280 ratio suggest contamination of the genomic material for the spectrophotometer reading (Introgen 2020; Lucena-Aguilar et al., 2015). For the RNA integrity test, the presence of two distinct bands suggests high quality RNA. Specifically, the top band is represented by 28S (rRNA), the middle band = 18S rRNA (Table 2; Figure 7). These methods helped determine whether or not RNA degradation of a replicate ensued. Specifically, the ribosomal RNA (rRNA) constitutes approximately 80% of total RNA and is therefore a valuable approach routinely employed to determine the integrity of a sample (ThermoFischer, 2022). Strongly contaminated RNA was discarded from the analysis.

Reverse Transcription. ~1 ug of RNA was converted into cDNA using the RT-kit (Table 3.1; iScript™ Reverse Transcription Supermix; BIORAD, 2020). This kit contains a RT supermix and a NO-RT control supermix. The NO-RT mix contains all the components of the iScript RT supermix except reverse transcriptase which was used to generate complementary DNA from an RNA template. The reverse transcription master mix (RTMM) for both conditions were prepared under specific conditions (Table 3.2, 3.3; BIORAD, 2020). Specifically, a total volume of 20uL was used for a single cDNA synthesis reaction. This volume contained 4uL of the corresponding RTMM (NO-RT or RT) along with 1ug of RNA template and the corresponding amount water for each reverse transcription reaction. Next, the reactions were incubated in a thermal cycle under specific conditions (Table 3.4; BIORAD, 2020).

Table 1. RNA Isolation Protocol (Prepared by: Idi Jeremie Shabani & Konrad Schottner)

Homogenization & Sample RNA extraction
1. Clean workspace using RNase Away or another chemical decontaminant, turn on centrifuge and set to 4˚C
2. Move tissue punches from -80˚C freezer, place on ice
3. Add 200uL of Trizol Reagent and homogenize the tissue thoroughly with a homogenizer ON ICE under the fume hood (carefully insert homogenizer to avoid spill over), make sure all tissue is dissolved a. the Volume of Trizol depends on the amount of tissue you use (1ml Trizol per 50-100mg tissue) b. 50 punches of brain tissue weigh approximately 4-5 mg
4. Let sit at RT for 5min
5. Add 20uL of chloroform per 100uL of Trizol used in each sample and cap (still in the fume hood)
6. Shake vigorously for 15s & incubate for 5 min at RT to permit complete dissociation of the
7. Centrifuge samples for 15min 12000xg at 4˚C
8. During the centrifugation, prepare (for each sample) a fresh RNAse-free tube chilled on ice
RNA precipitation
9. Once centrifugation is complete, transfer the aqueous phase (~100uL; clear supernatant) to the freshly prepared RNAse free tube under the fume hood (be extremely careful, do not touch of transfer any material from the interphase, repeat centrifugation step if you touch the interphase with the pipette tip.
10. Add 1uL of glycogen to the aqueous phase and gently mix by flicking the tube
11. Add 50uL of isopropanol per 100ul of Trizol
12. Invert tube(s) by hand 10-20x to mix
13. Incubate for 15min at RT
14. Centrifuge for 10min at 12000xg at 4°C to precipitate the RNA
15. Discard the supernatant with a pipette
16. Add 500uL of 75% EtOH (***EtOH must be made using DEPC water), invert tube gently
17. Centrifuge for 5min at 7500xg at 4°C
18. Discard the supernatant with a pipette, observe the pellet
19. Repeat steps 15-17 once or twice
20. Pulse spin & remove the remaining EtOH content by pipetting
21. Air dry the RNA pellet for ~5min (until pellet starts to become transparent), place on heat block for 30-60s at 37°C to completely evaporate EtOH, make sure the pellet does not dry for too long as it will affect solubility later
RNA solubilization
22. Resuspend the pellet in 30uL of DEPC treated water
23. Incubate at 37°C for 5-10 minutes & flick content every 1min, pulse spin when done *** PLACE SAMPLES ON ICE TO PREVENT DEGRADATION
24. Proceed with RNA concentration measurement & RNA integrity test
25. Proceed with cDNA synthesis (RT-PCR) when your RNA quality is good OR store at -80C
Nanodrop
- use 1ul to quantify RNA concentration twice (2 replicates)

Table 2. RNA Integrity Test (Aranda et al., 2012)

Reagents (for 100mL Agarose gel) 1g Agarose 1ml bleach solution 100 ml 1xTAE buffer 5ul Ethidiumbromide
Instructions
1. Weigh Agarose and transfer into a beaker
2. Measure the volume of 1xTAE buffer and transfer into beaker
3. Add bleach (1% v/v), mix gently and let sit for 5min, mix occasionally
4. Dissolve Agarose by heating the solution, make sure it is completely dissolved (BE CAREFUL, IT IS HOT)
5. Let the solution cool down a bit (but make sure it does not solidify)
6. Add the Ethidiumbromide to the solution (WEAR GLOVES, UNDER THE FUMEHOOD) and mix
7. Pour the solution into gel mold, remove all bubbles, add the comb and let it solidify
Running the Gel
Reagents: 1xTAE buffer (~700ml) - gel - RNA (1ug, but 500ng will work too if you have low yield) - 6xloading dye - 100bp ladder
8. Transfer gel into gel electrophoresis chamber, the top of the gel has to "face" the negative pole black), RNA (and DNA) moves towards the positive pole (red)
9. Remove comb
10. Pour TAE buffer into chamber so that it slightly covers the gel, make sure there is no bubble
11. Load the gel: a. 6ul of 100bp ladder b. 25ul of RNA (1ug, or 500ng just in case) mixed with loading dye c. -take the desired volume of solution that contains 1ug RNA (if your concentration is 1.5ug RNA/ul, you take 0.67ul), and add water to a total volume of 25ul d. -add 5ul of 6x loading dye (to a final concentration of 1x), mix by aspirating pipette iii. load 25ul into the pocket
12. Run the gel at 110V for no longer than 30min (15-20min is sufficient)
13. Once done, take the gel out of gel mold (carefully, do not break it) and wrap in plastic wrap foil
14. Image gel at the Kodak imaging station & save the file ***Exposure times (5-10s), slowly increase time if obtain weak signal.

iScript™ Reverse Transcription Supermix Protocol for RT-qPCR (BIORAD, 2020)

Table 3.1. Component employed for reaction mix

Reagent	Description
iScript RT Supermix	5x RT supermix with RNase H+ Moloney murine leukemia virus (MMLV) reverse transcriptase, RNase inhibitor, dNTPs, oligo(dT), random primers, buffer, MgCl2, and stabilizers
iScript No-RT Control Supermix	5x no-RT control supermix formulated to serve as a no-enzyme control, contains all components of iScript RT Supermix except reverse transcriptase
Nuclease-free water	--

Table 3.2. Reaction Setup for a Single cDNA synthesis Reaction

Component	Volume per Reaction, uL
iScript RT Supermix	4
RNA Template	5.4
Nuclease-free water	10.6
Total volume	20

Table 3.3. Reaction Setup for Multiple cDNA Synthesis Reactions

Component	Volume per Reaction, uL
iScript RT Supermix	48
Nuclease-free water	132
Total volume	180

Table 3.4. Reaction Protocol

Priming	5 min at 25C
Reverse Transcription	20 min at 46C
RT inactivation	1 min at 95C

qPCR analysis & Design (ie: Maestro). The mastermix and other frozen reaction components were thawed to room temperature. Each reaction was centrifuged for a short period of time to collect solutions at the bottom of tubes and then stored on ice protected from light. The qPCR reactions were prepared by adding all the required components (excluding template) under specific conditions (Table 4.1; SsoAdvanced Universal SYBR Green Supermix; BIORAD 2013). This mixture contained primers, water, and premixing reagents provided by the manufacturer to permit gene amplification. Homogeneity was ensured by thoroughly mixing the reagents and dispensing them in equal amounts in each PCR tube/plate. Each sample was diluted according to prior standard curve assessment (Table). Once this step is accomplished, the templates and the mastermix were added to the corresponding wells and sealed. The plate(s)/tube(s) were subsequently vortexed for ~30 seconds to ensure proper mixing of the reaction components and remove any air bubbles. The thermal cycling parameters were set under specific conditions (Table 4.2; SsoAdvanced Universal SYBR Green Supermix) and the plate was loaded onto the RT-PCR instrument to commence the run (BIORAD 2013). Once the run is finalized the data was analyzed using the CFX MAESTRO software.

In this experiment, two different groups were established to measure differential gene expression. The experimental group consisted of a homozygous (-/-) knockout of *Bmal1*, while the control group was a WT (+/+) counterpart. Primer3 was used to design appropriate primers and specific parameters were set for each primer pair (Biocenter 2013; Primer3, 2012). Both groups were treated with reverse transcriptase (RT) to produce complementary DNA (cDNA) from the RNA template. An additional condition was added and served as an additional control group consisting of no template (NTC). This control was employed to monitor for primer dimers and extraneous nucleic acid contaminations (QIAGEN 2013).

In this experiment, gene expression was normalized using the analysis tools from the software provided by CFX96 RT-Maeastro (BIORAD, 2013). The results were analyzed using the comparative threshold method (ΔΔCT) which assumes that the amplification efficiency is close to 100%. The threshold cycle (CT) refers to the cycle of amplification required for the fluorescent signal to cross the threshold[38]. In this technique the CT values are obtained from two different RNA experimental samples (WT and SKO), normalized to two housekeeping (HK) genes (*Gapdh* and *Hprt*) for reliability, then compared. Once these values are obtained, the difference between the Ct values of the targets and the HK are calculated (ΔCT) and the difference in the ΔCT values between each sample is also calculated (ΔΔCT). The fold change in expression of the targets in each experimental condition is represented by 2^(-ΔΔCt) (Livak & Schmittgen, 2001). Using this approach, we determined the relative expression of the experimental genes in this study.

Statistical Analysis. Microsoft Excel, and GraphPad Prism software were used for statistical analysis. Repeated Measure ANOVA's were conducted to determine whether there is a significant difference in gene expression between the (+/+) and (-/-) group at two different time points.

SsoAdvanced™ Universal SYBR Green Supermix Protocol for RT-qPCR (BIORAD, 2020)

Table 4.1. Reaction Setup for a Single cDNA synthesis Reaction

Component	Volume per 20uL Reaction	Final Concentration
SsoAdvanced universal SYBR® Green supermix (2x)	10	1x
Forward and reverse primers	2.6 each	300nM
Template	1 (serial dilution according to table 7)	cDNA: 100ng/uL
Nuclease-free H2O	3.7	--
Total reaction mix volume	20uL	--

Table 4.2. Thermal Cycling Protocol

Amplication Stages				
Polymerase Activation and DNA Denaturation	Denaturation at 95/98C	Annealing/Extension + Plate Read at 60C	Cycles	Melt-Curve Analysis
30 sec at 95C	10 sec	30 sec	40	65 – 95C 0.5C increment 3sec/step

RESULTS

RNA Isolation & Quantification (Spectrophotometry). In this experiment, we examined the differential gene expression across several conditions (ie: Wild Type – WT, Knockout – KO) of male and female transgenic mice bearing floxed alleles of the *Bmal1* gene. The first step to determining gene expression, was the isolation of RNA from the samples and the removal of genomic DNA to allow an accurate representation of the transcriptome. Once the RNA was purified, the absorbance of each sample was measured with the use of a spectrophotometer at varying wavelengths (230, 260, 280nm). The ratio of one absorbance unit was 40ng/ul of RNA. This value was employed to determine the RNA concentration of the samples. Using these values, the ratios of 260/230 (RNA vs. cell debris) and 260/280 (RNA vs. proteins) were calculated to accurately determine the quality and quantity of the samples. An absorbance ratio of 260/2

Following the quantification of the RNA sample, we were able to determine which replicate should be employed to perform the reverse transcription. This reaction was accomplished to produce cDNA libraries of the samples that were subsequently quantified with (RT-qPCR) to detect changes in gene expression. The 260/230 ratio was also assessed as a secondary measure of nucleic acid purity. A ratio of 2.0-2.2 is indicative of a pure RNA sample, while a value below that range for the 260/230 ratio suggested contamination of the genomic material for the spectrophotometer reading which absorbs at 230nm (Introgen 2020; Lucena-Aguilar et al., 2015).

RT-qPCR Data collection. In order to determine the significance of differential gene expression between conditions, the use of CFX Maestro (qPCR results) raw data files of CQ values were saved and transformed into an excel file. All statistical analyses were run using Microsoft Excel, while Prism 9 and Clustergrammer (Python) were used to validate analyses and generate graphs displaying changes in gene expression for each target (Figure 1, 2, 3, 4, 5, 6, 7). Essentially, the experimental condition consisted of male and female mice samples with a Bmal1 deletion (KO), while the control condition consisted of Wild Type male and female mice samples. For both groups, gene expression was examined at two different time points (ZT2 and ZT14). As such, we were able to determine the mean (CT) values for each group and target(s). Overall, our Ct values were relatively constant indicative of the low standard deviation (SD) for each sample. However, there were a few samples which produced a greater variation (large SD) suggesting these samples may have been degraded. These samples were removed as outliers can severely distort the data (Osbourne et al., 2004) . Thus, to correct and reduce the error variance reported in the Ct values, we removed the outliers (ie: samples with large SD) to allow for representative results and a normal distribution of scores in each variable of interest. Additionally, the threshold fluorescence levels of each target gene (*DRD2*, *MAOA*, *A2a*, *GABBR1*, and *GAD67*) was compared to the endogenous controls, Glyceraldehyde 3-phosphate dehydrogenase (*GAPDH)* and Hypoxanthine-guanine phosphoribosyltransferase (*HPRT)* at two different time points (ZT2 and ZT14) and the very same concentration for each condition (300nM). The ΔCT was calculated for each experimental condition (WT vs. KO) and normalized against the endogenous controls.

Molecular Data – Overview. 2 x 2 within-subjects ANOVAs were conducted to measure the level of mRNA expression of each target between genotypes (WT vs. KO) across two different time points (ZT2 and ZT14) in both male and female mice. All effects were non-statistically significant at the .05 significance level. Reported in table X1 and X2 (A-F) are descriptive statistics (ie: mean and standard deviation) for each genotype at both timepoints. The results for

the 2 x 2 within-subject ANOVAs of each target are found in Table X3 for males (A-F) and Tables X4 (A-F) for females.

GABBR1 **: Down-regulatory trend at each timepoint for (KO) Males and Females (all non-significant).** For males, the two-interaction between genotype and timepoint explains 0.11% of the total variability. A non-statistically significant difference was observed in the relative mRNA expression between the control (WT), and knockouts (KO) across the two different timepoints (ZT2 vs ZT14), $F(1, 6) = 0.007$, $p = 0.93$. Descriptive statistics indicated that the normalized gene expression of WT ($M = 1.13$) was higher than KO ($M = 0.90$). Furthermore, there was a trend toward *GABBR1* down-regulation observed in the (KO) at each timepoint; however, it did not reach statistical significance. A lower down-regulatory trend was observed at (ZT2). Specifically, the normalized gene relative expression was lower in the subjective day (ZT2: $M = 0.93$) in comparison to the subjective night (ZT14: $M = 1.10$), irrespective of genotype (See Figure 2A). Post-hoc results showed no statistically significant differences (See Table A3).

With respect to female mice, the two-way interaction between genotype and timepoint explains 1.01% of the total variability. A non-statistically significant difference was observed in the relative mRNA expression between the control (WT), and knockouts (KO) across the two different timepoints (ZT2 vs ZT14), $F(1, 8) = 0.1190$, $p = 0.74$. Descriptive statistics indicated that the normalized gene expression of WT ($M = 0.96$) was higher than KO ($M = 0.75$), irrespective of genotype. Similarly, there was a trend toward *GABBR1* down-regulation observed in the (KO) for females at each timepoint; however, it did not reach statistical significance. In contrast, a lower down-regulatory trend was observed at (ZT14). Specifically, the normalized gene relative expression was higher in the subjective day (ZT2: $M = 0.88$) in comparison to the subjective night (ZT14: $M = 0.83$), irrespective of genotype (See Figure 2B). Post-hoc results showed no statistically significant differences (See Table A4).

*GAD67***: Down-regulatory trend in Male (KO) at each timepoint; Up-regulatory trend in Female (KO) at each timepoint (all non-significant).** For males, the two-interaction between genotype and timepoint explains 7.48% of the total variability. A non-statistically significant difference was observed in the relative mRNA expression between the (WT), and (KO) across the two different timepoints (ZT2 vs ZT14), $F(1, 6) = 0.9421$, $p=0.37$. Descriptive statistics indicated that the normalized gene expression of WT ($M = 1.64$) was higher than KO ($M = 0.83$). Furthermore, there was a trend toward *GAD67* down-regulation observed in the (KO) at each timepoint; however, it did not reach statistical significance. A lower down-regulatory trend was observed at (ZT14). Additionally, it was observed that the normalized gene expression was lower in the subjective day (ZT2: $M = 0.89$) in comparison to the subjective night (ZT14: $M = 1.56$), irrespective of genotype (See Figure 3A). Post-hoc results showed no statistically significant differences (See Table B3).

With respect to female mice, the two-way interaction effect between genotype and time point explains about 1.85% of the total variability. No statistically significant differences were observed in the percentage of time spent in the open arms between (WT) and (KO) across the two different time points (ZT2 vs ZT14), $F(1, 8) = 0.1608$, $p =0.70$. Descriptive statistics indicated that the normalized gene relative expression of WT ($M = 0.98$) was lower than KO ($M = 1.16$). Furthermore, there was a trend toward *GAD67* up-regulation observed in the (KO) at each timepoint; however, it did not reach statistical significance. A higher up-regulatory trend was observed at (ZT14) in (KO). Specifically, it was observed that the normalized gene expression was lower in the subjective day (ZT2: $M = 1.04$) in comparison to the subjective night (ZT14: $M = 1.10$) for the (KO) genotype only (See Figure 3B). Post-hoc results showed no statistically significant differences (See Table B4

A2a: **Down-regulatory trend at ZT2 in (KO) for each sex; Up-regulatory trend at ZT14 in (KO) for each sex (all non-significant).** For males, the two-interaction between genotype and timepoint explains 13.40% of the total variability. A non-statistically significant difference was observed in the relative mRNA expression between the (WT), and (KO) across the two different timepoints (ZT2 vs ZT14), $F(1, 6) = 0.9321$, $p=0.37$. Descriptive statistics indicated that the normalized gene expression of WT ($M = 0.96$) was lower than KO ($M = 1.16$). Furthermore, there was a trend toward *A2a* down-regulation observed in the (KO) at (ZT2), while an up-regulatory trend was observed in the same genotype at (ZT14). Each trend did not reach statistical significance. A lower down-regulatory trend was observed at (ZT2). Specifically, it was observed that the normalized gene expression was lower in the subjective day (ZT2: $M = 0.99$) in comparison to the subjective night (ZT14: $M = 1.13$) for the (KO) genotype only (See Figure 4A). Post-hoc results showed no statistically significant differences (Table C3).

With respect to female mice, the two-way interaction between genotype and timepoint explains 13.45% of the total variability. No statistically significant differences were observed in the percentage of time spent in the open arms between (WT) and (KO) across the two different time points (ZT2 vs ZT14), $F (1, 8) = 1.617$, $p = 0.24$. Descriptive statistics indicated that the normalized gene relative expression of WT ($M = 0.93$) was higher than KO ($M = 0.63$). Furthermore, there was a trend toward *A2a* down-regulation observed in the (KO) at (ZT2), while an up-regulatory trend was observed in the same genotype at (ZT14). Each trend did not reach statistical significance. Additionally, it was observed that the normalized expression was higher in the subjective day (ZT2: $M = 1.01$) in comparison to the subjective night (ZT14: $M = 0.55$) for the (KO) genotype only (See Figure 4B). Post-hoc results showed no statistically significant differences (See Table C4).

DRD2: **Up-regulatory trend in Male (KO) at each timepoint; Mis-regulation trends in Female (KO) (all non-significant).** For males, the two-interaction between genotype and timepoint explains 0.79% of the total variability. A non-statistically significant difference was observed in the relative mRNA expression between the (WT), and (KO) across the two different timepoints (ZT2 vs ZT14), $F (1, 6) = 0.051$, $p=0.83$. Descriptive statistics indicated that the gene relative expression of WT ($M = 1.16$) was lower than KO ($M = 1.35$). Furthermore, there was a trend toward *DRD2* up-regulation observed in the (KO) at each timepoint; however, it did not reach statistical significance. Additionally, it was observed that the normalized gene expression was lower in the subjective day (ZT2: $M = 1.16$) in comparison to the subjective night (ZT14: $M = 1.34$), irrespective of genotype (See Figure 5A). Post-hoc results showed no statistically significant differences (See Table D3).

With respect to female mice, the two-interaction between genotype and timepoint explains 14.13% of the total variability. A non-statistically significant difference was observed in the relative mRNA expression between the (WT), and (KO) across the two different timepoints (ZT2 vs ZT14), $F (1, 8)= 1.636$, $p=0.24$. Descriptive statistics indicated that the normalized gene expression of WT ($M = 1.80$) was lower than KO ($M = 2.52$). Furthermore, there was a trend toward *DRD2* down-regulation observed in the (KO) at (ZT14), while an up-regulatory trend was observed at (ZT2). Each trend did not reach statistical significance. Specifically, it was observed that the normalized gene expression was lower in the subjective day (ZT2: $M = 1.92$) in comparison to the comparison to the subjective night (ZT14: $M = 2.41$) in (WT). Interestingly, the inverse of this relationship was seen in the (KO) group (See Figure 5B). Post-hoc results showed no statistically significant differences. (See Table D4)

MAOA: **Differences in mis-regulation trends for each sex (all non-significant).** For males, the two-interaction between genotype and timepoint explains 0.21% of the total variability. A non-statistically significant difference was observed in the relative mRNA expression between the (WT), and (KO) across the two different timepoints (ZT2 vs ZT14), F (1, 6) = 0.0145, p=0.91. Descriptive statistics indicated that the normalized gene relative expression of WT (M = 1.14) was higher than KO (M = 1.12). Furthermore, there was a trend toward *MAOA* up-regulation observed in the (KO) at (ZT14), while a down-regulatory trend was observed at (ZT2). Each trend did not reach statistical significance. Specifically, it was observed that the normalized gene expression was lower in the subjective day (ZT2: M = 0.98) in comparison to the subjective night (ZT14: M = 1.29), irrespective of genotype (See Figure 6A). Post-hoc results showed no statistically significant differences (See Table E3).

With respect to female mice, the two-interaction between genotype and timepoint explains 1.46% of the total variability. A non-statistically significant difference was observed in the relative mRNA expression between the (WT), and (KO) across the two different timepoints (ZT2 vs ZT14), F (1, 8)= 0.1203, p=0.74. Descriptive statistics indicated that the normalized gene relative expression of WT (M = 1.00) was higher than KO (M = 0.98). Furthermore, there was a trend toward *MAOA* down-regulation observed in the (KO) at (ZT14), while an up-regulatory trend was observed at (ZT2). Each trend did not reach statistical significance. Specifically, it was observed that the normalized gene expression was higher in the subjective day (ZT2: M = 1.01) in comparison to the subjective night (ZT14: M = 0.98) for the (KO) genotype only (See Figure 6B). Post-hoc results showed no statistically significant differences (See Table E4).

A)

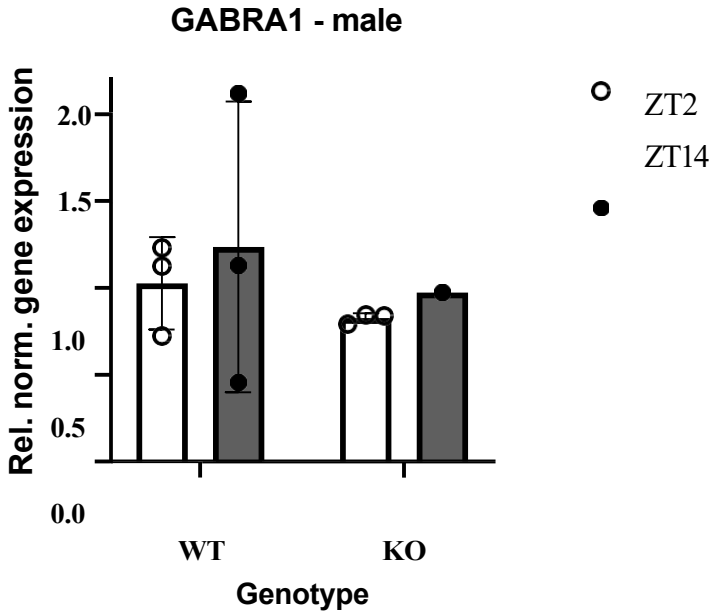

B)

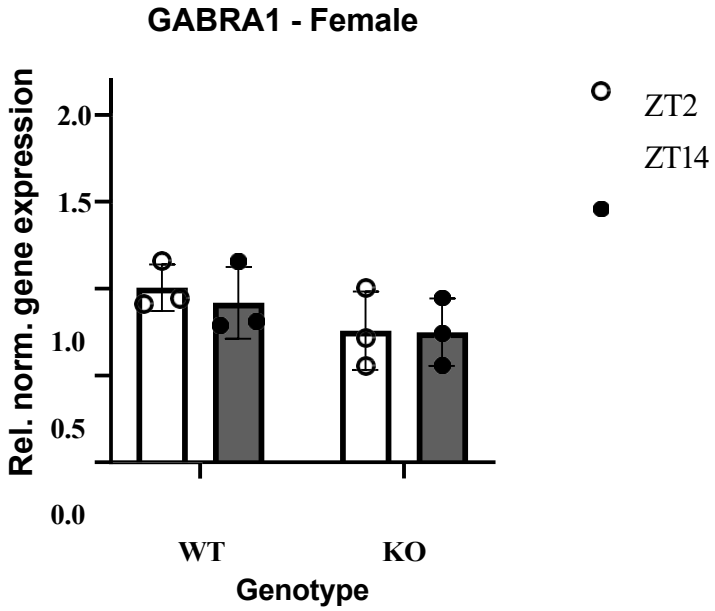

Figure 2. Relative mRNA expression of *GABBR1* in male and female mice at two different time points (ZT2 & ZT14). (A) In males, no significant differences were observed on the genotype variable between WT (n = 3) and KO (n = 1) across the two time points for *GABBR1*. A down-regulation of *GABBR1* was observed between timepoints following *Bmal1* deletion. (B) In females, there were no significant differences observed in the genotype variable between WT (n = 3) and KO (n = 3) across the two time points for GABBR1. Similarly, a down-regulation of GABBR1 was observed at each timepoint following Bmal1 deletion. Errors bars represent the standard error of the mean.

A)

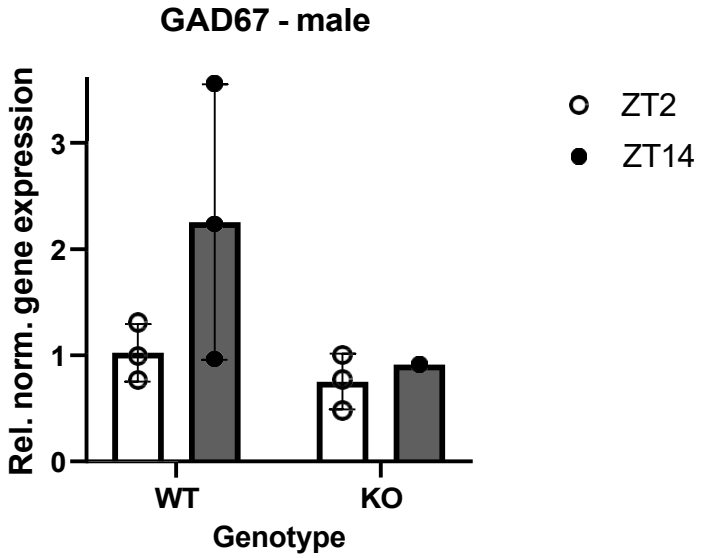

B)

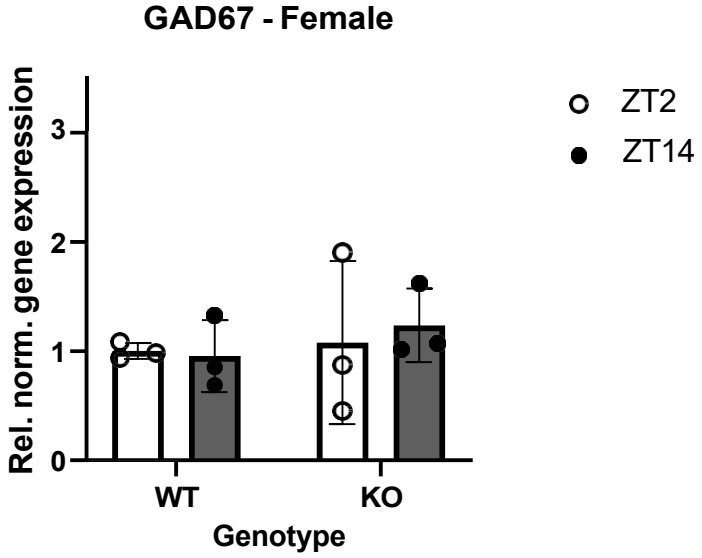

Figure 3. Relative mRNA expression of *GAD67* in male and female mice at two different time points (ZT2 & ZT14). (A) In males, no significant differences were observed on the genotype variable between WT (n = 3) and KO (n = 1) across the two time points for GAD67. A down-regulation of *GAD67* was observed in the (KO) group following Bmal1 deletion. (B) In females, there were no significant differences observed in the genotype variable between WT (n = 3) and SKO (n = 3) across the two time points for the *GAD67* gene. An up-regulation of *GAD67* was observed in (KO) at each timepoint following Bmal1 deletion. Error bars represent the standard error of the mean.

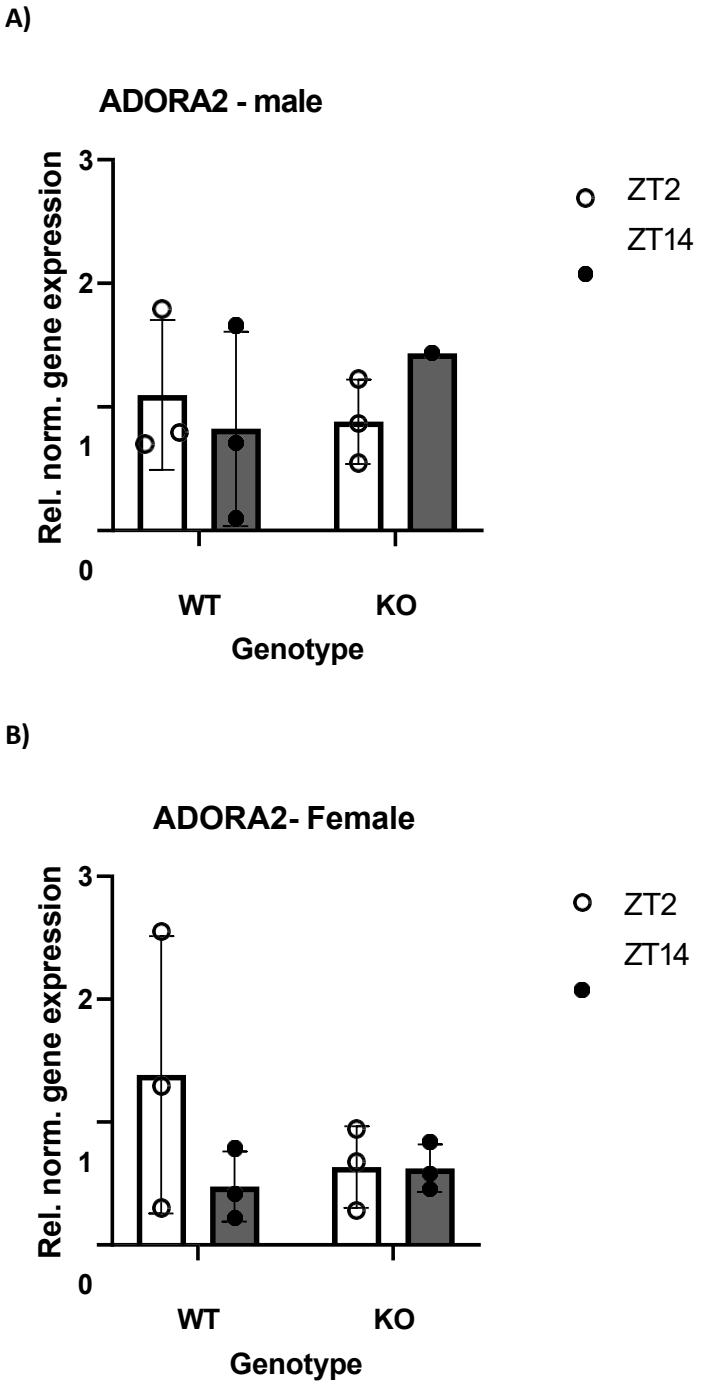

Figure 4. Relative mRNA expression of *A2a* in male and female mice at two different time points (ZT2 & ZT14). (A) In males, no significant differences were observed on the genotype variable between WT (n = 3) and KO (n = 1) across the two time points for *A2a* following Bmal1 deletion. A down-regulation of *A2a* was observed in the (KO) group in the subjective day (ZT2), while an up-regulation of *A2a* was observed in the (KO) group in the subjective night (ZT14). (B) In females, no significant differences observed in the genotype variable between WT (n = 3) and KO (n = 3) across the two time points for the *A2a* gene. Similarly, a downregulation of *A2a* was observed in the (KO) group in the subjective day (ZT2), while an upregulation was observed in the (KO) group in the subjective night (ZT14). Error bars represent the standard error of the mean.

A)

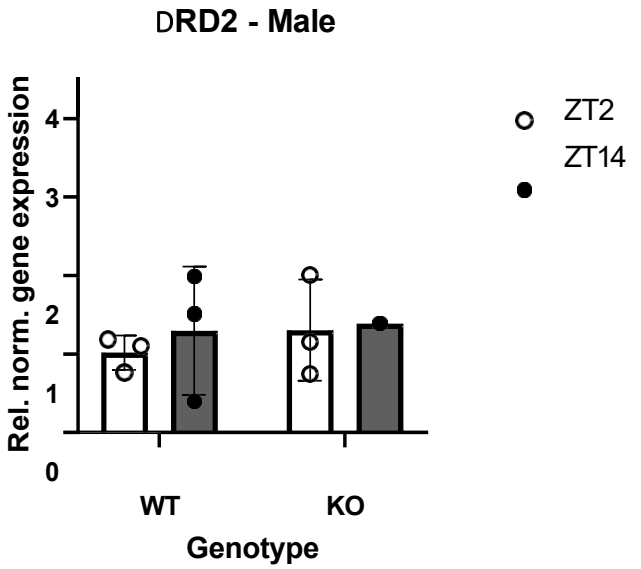

B)

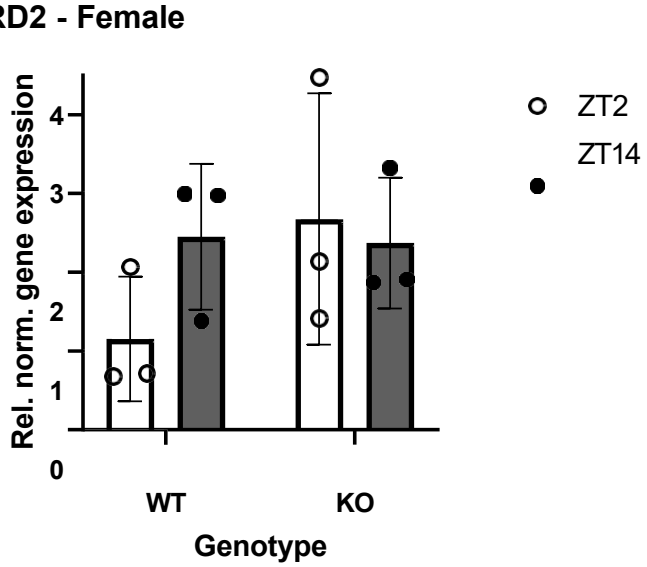

Figure 5. Relative mRNA expression of *DRD2* in male and female mice at two different time points (ZT2 & ZT14). (A) In males, no significant differences were observed on the genotype variable between WT (n = 3) and KO (n = 1) across the two time points. An up-regulation of *DRD2* was observed in (KO) at each timepoint following Bmal1 deletion. (B) In females, there were no significant differences observed in the genotype variable between WT (n = 3) and SKO (n = 3) across the two time points. An up-regulation of *DRD2* at ZT2 was observed in the (KO) group following Bmal1 deletion in the (KO), while a down-regulation of *DRD2* at ZT14 was observed in the (KO) group. Specifically, the relative expression of *DRD2* was moderately higher in the subjective day (ZT2), while the relative normalized expressed was slightly lower in the subjective night. Error bars represent the standard error of the mean.

A)

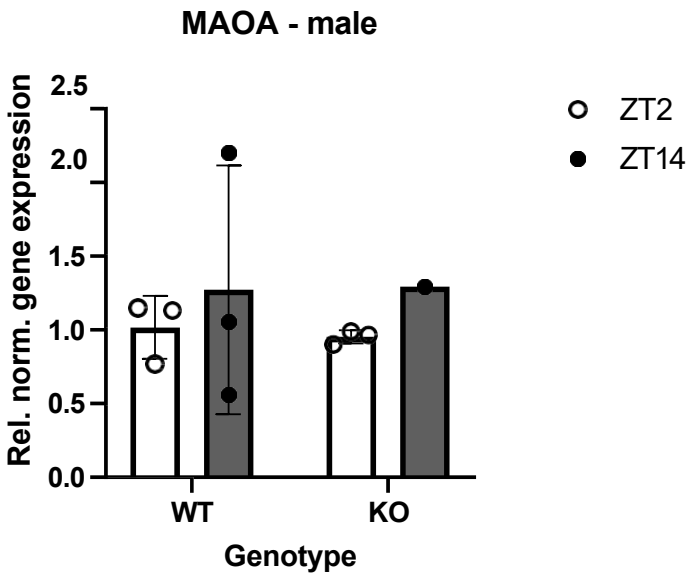

B)

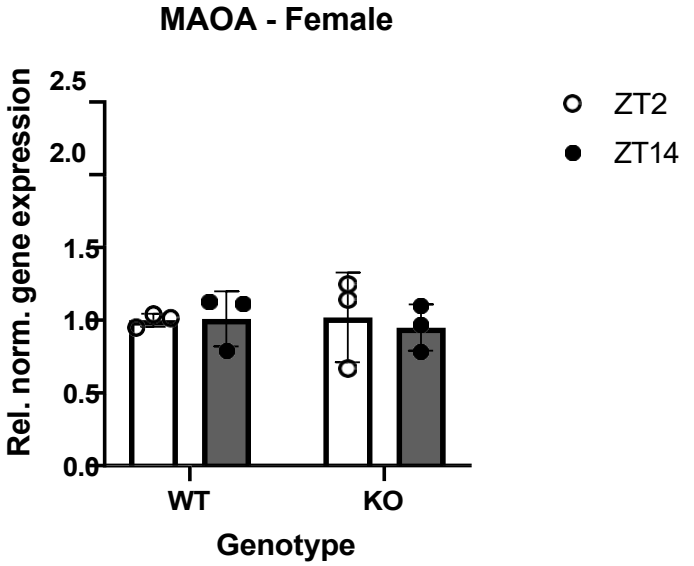

Figure 6. Relative mRNA expression of *MAOA* in male and female mice at two different time points (ZT2 & ZT14). (A) In males, no significant differences were observed on the genotype variable between WT (n = 3) and KO (n = 1) across the two time points following Bmal1 deletion. A down-regulation of *MAOA* was observed in the (KO) group in the subjective day (ZT2), while an up-regulation of *MAOA* was observed in the (KO) group in the subjective night (ZT14). (B) In females, there were no significant differences observed in the genotype variable between WT (n = 3) and KO (n = 3) across the two time points. An up-regulation of *MAOA* was observed in the (KO) group in the subjective day (ZT2), while a down-regulation of *MAOA* was observed in the (KO) group in the subjective night (ZT14). Error bars represent the standard error of the mean.

DISCUSSION

The influence of the field of circadian physiology in neuropsychiatric and neurodegenerative disorders is continuously developing. Therefore, advancements in the scientific and clinical community have been crucial in exploring ways to assess the role of various brain regions, and the underlying mechanisms that associate clock genes to mood disorders. One brain region of interest is the striatum, which has been implicated in depression and anxiety (McClung 2019). In this project, we developed a unique mouse line with a striatal clock gene deletion to evaluate the effect of a clock manipulation on the expression of Glutamatergic, Dopaminergic and GABAergic receptors in the dorsal striatum of male and female mice. The observations from this project partially support the hypothesis that deletion of *Bmal1* in striatal MSNs will affect the gene expression of the selected candidates. This is because the trends observed in the gene expression profile were of non-statistical significance suggesting additional studies are required to further evaluate the effect(s) of clock manipulations on neurotransmission. Interestingly, different mis-regulation trends (up- and down-regulation) were observed in the targets selected.

First, we wanted to determine whether *Bmal1* deletion affects the expression of *GABBR1*. It is a major inhibitory neurotransmitter in the mammalian brain that plays a role in mood disorders and the principal neuron in the striatum (Li et al., 2019). A down-regulatory trend on *GABBR1* expression at each timepoint (ZT2 and ZT14), for males and females (WT vs. KO) was observed. Each trend did not have statistical significance. This suggests *Bmal1* knockdown potentially mediates negative regulation of *GABBR1* transcription. The relative gene expression was higher in the subjective nighttime for males (ZT14-KO), while it was higher in the subjective day time (ZT2-KO) for females. These results are in line with concurrent literature where it was found that NPAS2 significantly reduced the expression of *GABBR1* at two timepoints (ZT4 and ZT16) in male mutant mice with a viral-mediated knockdown in the NAc (Ozburn et al., 2017). Interestingly, the NPAS2 protein can dimerize with *Bmal1* and is analogous in function to the CLOCK protein in the TTFL highlighting its relevance. Additionally, depletions of *GABBR1* in the prefrontal cortex, a brain region closely related to the striatum that also affects executive functioning, is associated with deficits in reward-learning in mice. In line with this documentation, a group observed transient downregulation of *GABBR1* in the dorsal striatum of rats that were place-conditioned to methamphetamine only (Jiao et al., 2016). This collective evidence suggests that *Bmal1* deletion may play a role in the dysregulation of *GABBR1*, a target which has been associated with the development of neuropsychiatric disorders and addiction (Karatsoreos, 2014; Ozburn et al., 2017). Therefore, the association between *GABBR1* and Bmal1 deletion must be further examined.

Second, we sought to further examine Glutamate signaling in the striatum. Specifically, we assessed *GAD67* expression following *Bmal1* deletion, a rate limiting enzyme that synthesizes GABA and is found in several brain regions (ie: striatum). Dysregulation of *GAD67* expression has been associated with several mood disorders such as schizophrenia (McClung et al., 2013; Karatsoreos, 2014). Furthermore, previous studies have shown that glutamatergic transmission provides stimulation to GABAergic neurons thereby modulating inhibitory output. Therefore, we wanted to determine whether Bmal1 mediates the expression of *GAD67*. A down-regulatory trend was observed in *GAD67* expression in Male (KO) at each timepoint suggesting negative regulation of *GAD67* transcription. In contrast, an up-regulatory trend in *GAD67* expression was observed at each timepoint in females following Bmal1 deletion suggesting positive regulation of *GAD67* transcription. These results indicate that Bmal1 knockdown had different effects on *GAD67* expression depending on sex, suggesting sex-specific differences

may play a role in the transcriptional regulation of *GAD67*. Similarly, this notion was also revisited by experts who investigated mice with a *Bmal1* deletion. The results showed that circadian clock genes such as Bmal1 can affect ethanol consumption in a sexually dimorphic manner (De Zavalia et al., 2020). Specifically, the alcohol intake increased in males, while a repression was seen in females. Further in line with this phenomenon, a group of experts observed that there was generally a significant higher expression of GAD67 in female schizophrenic cases while this association was not seen in males (Bristow et al., 2015; Lindberg et al., 2018). This sex-specific preference may be attributed to the possible interaction between Bmal1 and Per2 or other constitutive factors and must be further investigated to determine the exact underlying mechanism(s) affecting transcriptional regulation of *GAD67*.

Third, we sought to examine whether *Bmal1* deletion affects the expression of *A2a*. It is a receptor that is expressed in the brain and plays an important role in the regulation of glutamate and dopamine (DA) release thereby influencing the development of mood disorders (Medline 2020). The results indicated that upon *Bmal1* knockdown, a down-regulatory trend of *A2a* expression at (ZT2) in each sex was observed. In contrast, an up-regulatory trend was observed in male and female (KO) at (ZT14). These observations suggest that *Bmal1* knockdown had different effects on *A2a* expression depending on timepoint, indicating diurnal differences may play a role in the transcriptional regulation of *A2a*. Interestingly, the normalized gene expression was lower in the subjective day in comparison to the subjective night in male and female (KO). These diurnal differences in expression found in males and females (WT and KO) are in line with concurrent literature in which compromising expression (up- and down-regulation) were observed in male mice (Lindberg et al., 2018; Sanchez, 1995). Specifically, there was a peak of adenosine early during the circadian night, while its lowest expression was observed during the day (approximately ZT6; Lindberg et al., 2018; Sanchez, 1995).

Fourth, we sought to investigate whether *Bmal1* deletion affects the expression of *DRD2*. Dopamine provides robust rhythmic signals to the striatum which in turn may impact the development of neuropsychiatric disorders (Ozburn et al., 2017; Korshunov et al., 2017). This is because rhythms in clock gene expression are sensitive to changes in dopamine, and as such, may play a role in modulating circadian activities in the striatum, specifically, DRD2. These receptors play a vital role in modulating physiological functions related locomotion, hormone production and addiction (Usiello et al., 2000; Hood et al., 2010). The results indicated that upon *Bmal1* deletion, an up-regulatory trend of *DRD2* expression was observed in male (KO) at each timepoint suggesting positive regulation. Interestingly, it was observed that the normalized gene expression was lower in the subjective day in comparison to the subjective night irrespective of genotype. In contrast, in females with a *Bmal1* deletion mis-regulatory trends were observed. Specifically, a *DRD2* up-regulatory trend was only observed at (ZT2), while a down-regulatory trend of *DRD2* expression was observed at (ZT14). Similarly, it was observed that the normalized gene expression was lower in the subjective day in comparison to the subjective night irrespective of genotype. These diurnal differences in expression found in males and females (WT and KO) are in line with previous literature in which compromising expression (up- and down-regulation) of *DRD2* were observed in male mice following *Npas* knockdown (Ozburn et al., 2015; Ferris et al., 2014). Specifically, Npas2 knockdown significantly abolished *DRD2* diurnal expression in the NAc. Interestingly, the same group showed that cocaine treatment did not significantly affect diurnal variation of *DRD2* (Ferris et al., 2014). These observations are different from previous literature which has suggested that DRD2 gene expression is upregulated in the striatum and PFC of addicted mice (Williams et al., 2021). Based on this conflicting evidence, the role of *Bmal1* deletion in the dysregulation of *DRD2*

must be further examined to elucidate a clearer understanding of its molecular mechanism, and whether sex-specific differences apply (Williams et al., 2021).

Finally, we sought to examine whether *Bmal1* deletion affects the expression of *MAOA*. It is an enzyme that has been associated with various mood disorders, plays a role in dopamine metabolism, and is clock-controlled (Domingo-Rodriguez et al., 2020; Medline 2020). The results suggest that upon Bmal1 deletion, many differences in mis-regulation trends were observed in each sex. Specifically, in male (KO), a down-regulatory trend of *MAOA* expression was observed at (ZT2), while an up-regulatory trend of *MAOA* expression was observed in the subjective night (ZT14). Interestingly, the inverse of this relationship was seen in females upon *Bmal1* deletion suggesting another sex-specific difference. Specifically, a down-regulatory trend of *MAOA* expression was observed in the subjective night (ZT14), while an up-regulatory trend of *MAOA* was observed in the subjective day (ZT2). Each trend did not have statistical significance. These results suggest Bmal1 may mediate the regulation of *MAOA* in a time-dependent fashion in the dorsal striatum. These observations are supported by previous literary evidence suggesting that the clock components *Bmal1/NPAS2* directly regulated *MAOA* transcription in a circadian fashion (Hampp & Albrecht, 2008; Laloum & Robinson-Rechavi., 2020). Specifically, the highest expression was seen in the light phase (ZT6), while the lowest was observed in the dark phase (ZT18). Additionally, in mice lacking *PER2*, both *MAOA* mRNA and protein levels were decreased further supporting the notion that degradation of monoamines is regulated by the circadian clock (Hampp & Albrecht, 2008).

Caveats

A potential limitation to our study is the relatively small sample size employed due to the current pandemic situation. This may have altered the significance of our findings obtained for the differential expression of our targets. Additionally, there are not enough timepoints to reveal the full effects of *Bmal1* gene deletion. To circumvent these issues, the use of more time points targets, and a larger sample will be required in future experiments to produce more representative results. This is because fewer time points per cycle contribute to a weaker detection of rhythmic patterns even if the transcriptome profiling quality is better (Laloum & Robinson-Rechavi). These subtle changes will allow us to more closely examine whether there are significant differences between the genotypes, and the role of *Bmal1* deletion in the dysregulation of the targets of interest.

Secondly, the use of more housekeeping (HK) genes should be used in future experiments to determine the most suitable selection. These genes are required for the basic cell maintenance and appropriate HK genes will express stable expression in varying conditions (ie: WT vs. KO; Levanon, 2014). While our experimental design did satisfy this condition, only two HK genes (*Gapdh* and *Hprt*) were employed in our experiment, the minimum required standard to allow for reliable results in RT-qPCR (Jain et al., 2018). Perhaps the use of more (HK) genes could have provided us with better candidates which in turn could further explain changes or patterns in the expression profile of the target genes.

Additionally, the use of other genetic editing approaches such as CRISPR/cas9 could have been employed to complement crelox technology. The employment of these methods has proven to be an invaluable tool in the field of molecular biology due to their numerous applications (ie: gene deletion or, gene knock in). They have allowed experts to assess the underlying mechanism of various pathologies and provide them with novel interventions to improve the prognosis of patients (Patmanathan et al., 2018).

Overall, the results obtained from this study provide insights into the physiology of the dorsal striatum and provides information about the molecular mechanisms which affects the brain. Specifically, the circadian rhythms and genes that make up the molecular clock play an important role in the expression of mood-related symptoms in psychiatric disorders. This study allows us to link Bmal1 to anxiety-like behavior, regulation of specific GABAergic, glutamatergic and dopaminergic expression in the dorsal striatum. Thus, despite some limitations, this study has clear implications and future directions it could visit.

Future Directions: Circadian physiology & biomedical link

In this experiment, we did not see significant differences in gene expression between timepoints and genotypes at the molecular level. Therefore, further investigation is warranted to examine differences concerning the underlying mechanisms by which circadian clock gene manipulation affect neurotransmission. Previous literature has observed that changes in rhythmicity could be a potential precursor or consequences of a condition (Fernandez et al., 2019). Thus, it is evident that disrupted circadian rhythms are a precursor and symptom of various psychiatric disorders (Ketchesin & McClung, 2018).

Hence, further studies will be imperative to investigate the modulatory role that circadian rhythms plays in behavioral output. Specifically, genetic studies will help elucidate the role(s) of individual circadian clock genes in mood regulation. Likewise, human work is required to complement the established mechanistic links that might underlie association between disrupted rhythms and a given condition. Thus, the implementation of longitudinal studies must be utilized to establish the temporal relationship between circadian disruption and outcomes (ie:like depression, cancer, or cardiovascular disease). This will also help determine whether other unknown factors influence the expression of clock genes.

Furthermore, subsequent studies could screen the nucleotide polymorphism (SNP) of clock genes associated with a specific psychiatric disorder and see how it affects MSNs functioning. For instance, using CRISPR/Cas9 we could create similar SNPs in rodents (albeit different sequence) OR do a large-scale study behaviorally screening rodents and sequencing each animal with behavioral abnormalities (Kim et al., 2021; Eckel-Mahan & Sassone-Corsi, 2013). This could be accomplished using a combination of RNAseq (or microarray) and bioinformatics to provide a transcriptome investigation of the genes affected by striatal deletion of core clock genes (ie:*Bmal1*). Ultimately, this presents a future in which we may be able to develop novel treatments for several diseases using different genomic approaches whether independently or in combination (ie: RNAseq, CRISPR/Cas9) to target various disorders associated with a specific genetic modification. Such studies will elucidate a clearer role on the influence of clock-controlled genes with relation to not only GABAergic, Glutamatergic, and Dopaminergic receptors, but also other relevant targets.

REFERENCES

1. Albrecht, U. (2012). Timing to perfection: the biology of central and peripheral circadian clocks. Neuron, 74(2), 246–260.
2. Albrecht U., (2013) Circadian Clocks and Mood-Related Behaviors. Accessed at: https://www.unifr.ch/biochem/assets/files/albrecht/publications/Albrecht2013.pdf
3. Aranda, SP., Lajoie, D., Jorcyk, CL (2012). Nucleic Acids.Eletrophoresi. Volume 33, Issue 22. 366-369.doi: 10.1002/elps.201100335
4. Biocenter TATAA (2013). Gene Expression Profiling: qPCR Toolkit for Quality Control. Accessed at: https://www.gene-quantification.de/qpcr-ngs-2013/posters/P105-qPCR-NGS-2013
5. BioRad (2020). iScript Reverse Transcription Supermix for RT-qPCR. Protocol
6. BioRad (2013). SsoAdvanced Universal SYBR Green Supermix. Protocol
7. Bordyugov, I. et al., (2018) Tuning the phase of circadian entrainment
8. Brambilla P., Perez J., Barale F., Schetttni G., Soares JC (2003) GABAergic dysfunction in mood disorders. Molecular Psychiatry. 8,721-737
9. Bozek, K., Relógio, A., Kielbasa, S. M., Heine, M., Dame, C., Kramer, A., et al. (2009). Regulation of Clock-Controlled Genes in Mammals. PLoS ONE 4, e4882. doi:10.1371/journal.pone.0004882
10. Bristow, GC., Bostrom, JA., Haroutunian V., Sodhi MS. (2015) Sex differences in GABAergic gene expression occur in the anterior cingulate cortex in schizophrenia. 167(0): 57–63. doi:10.1016/j.schres.2015.01.025
11. Carter, M., Sheih, J. (2015) Biochemical Assays and Intracellular Signaling. Guide to Research Techniques in Neuroscience (Second Edition)
12. Chi-Castaneda D., Ortega A. (2018). Circadian Regulation of Glutamate Transporters. doi: 10.3389/fendo.2018.00340
13. Chiou, YY., Yang, Y., Naim, R., Rui, Y., Selby CP., Sancar, A. (2016) Mammalian Period represses and de-represses transcription by displacing CLOCK-BMAL1 from promoters in a Cryptochrome-dependent manner. Oct 11;113(41):E6072-E6079. doi: 10.1073/pnas.1612917113. Epub 2016 Sep 29.
14. De Zavalia, N. et al. (2020). Sexually dimorphic influence of the circadian clock gene Bmal1 in the striatum on alcohol intake. bioRxiv. doi:10.1101/2020.09.16.299842
15. Domingo-Rodriguez et al., (2020). A specific prelimbic-nucleus accumbens pathway controls resilience versus vulnerability to food addiction.
16. Eckel-Mahan, K., Sassone-Corsi, P. (2013). Metabolism and the Circadian Clock Converge. Physiol Rev. 2013 Jan; 93(1): 107–135.doi: 10.1152/physrev.00016.2012
17. Falcon., A., Angela Ozburn,Shibani Mukherjee,Kole Roybal,Colleen A. McClung (2013). Differential Regulation of the Period Genes in Striatal Regions following Cocaine Exposure. Accessed at: https://doi.org/10.1371/journal.pone.0066438
18. Ferris, M. J., España, R. A., Locke, J. L., Konstantopoulos, J. K., Rose, J. H., Chen, R., et al. (2014). Dopamine transporters govern diurnal variation in extracellular dopamine tone. Proc. Natl. Acad. Sci. U.S.A. 111, E2751–2759.doi: 10.1073/pnas.1407935111
19. Hampp G., Albrecht., U (2008) The Circadian clock and mood-related behaviour. Communicative & Integrative Biology 1:1, 1-3;
20. Hampp, G., Ripperger, J. A., Houben, T. et al. (2008). Regulation of monoamine oxidase A by circadian-clock components implies clock influence on mood. Current Biology, 18(9), 678–683. doi:10.1016/j.cub.2008.04.012

21. Harbour, V. L., Weigl, Y., Robinson, B. & Amir, S. Phase differences in expression of circadian clock genes in the central nucleus of the amygdala, dentate gyrus, and suprachiasmatic nucleus in the rat. PLoS One 9, e103309, doi:10.1371/journal.pone.0103309 (2014).
22. He, S., Zhang X., Qu S. (2018) Glutamate, Glutamate Transporters, and Circadian Rhythm Sleep Disorders in Neurodegenerative Diseases. ACS Chem Neuroscience. doi: 10.1021/acschemneuro.8b00419
23. Health Canada (2020). Data Blog: Mental Illnesses in Canada. Accessed at: https://health-infobase.canada.ca/datalab/mental-illness-blog.html#:~:text=1%20in%203,illness%20during%20their%20lifetime%202
24. Hood et al., (2010). Endogenous dopamine regulates the rhythm of expression of the clock protein PER2 in the rat dorsal striatum via daily activation of D2 dopamine receptors. DOI: 10.1523/JNEUROSCI.2128-10.2010
25. Ikeda, Y., Y, Kinoshita Y, Kitajima T, Yoshimura R, Hashimoto S, O'Donovan MC, Nakamura J, Ozaki N, Iwata N. (2018). Variants of dopamine and serotonin candidate genes as predictors of response to risperidone treatment in first-episode schizophrenia. Oct;9(10):1437-43. doi: 10.2217/14622416.9.10.1437.
26. Invitrogen (2020). Trizol Reageant RNA Extraction Protocol
27. Jamwal S., Kumar P., (2019) Insight into the Emerging Role of Striatal Neurotransmitters in the Pathophysiology of Parkinson's Disease and Huntington's Disease: A Review doi: 10.2174/1570159X16666180302115032
28. Jain et al., (2018) Validation of house-keeping genes for normalization of gene expression data during diurnal/circadian studies in rice by RT-qPCR. Scientific Reports volume 8, Article number: 3203
29. Jiao et al,. (2016). Involvement of dorsal striatal α1-containing GABAA receptors in methamphetamine-associated rewarding memories. https://doi.org/10.1016/j.neuroscience.2016.02.001
30. Karatsoreos. I., (2014). Links between Circadian Rhythms and Psychiatric Disease. Front Behav Neuro. 8:162. lifespan. Nat Rev Neurosci. 2019 Jan; 20(1): 49–65.doi: 10.1038/s41583-018-0088-y
31. Kervezee L., Kosmadopoulos A., Boivin DB., (2018) Metabolic and cardiovascular consequences of shift work: The role of circadian disruption and sleep disturbances. DOI: 10.1111/ejn.14216
32. Ketchesin, Becker-Trail, McClung, (2018) Mood-related central and peripheral clock. DOI: 10.1111/ejn.1425
33. Kim, M. et al. (2017). Neurobiological functions of the period circadian clock 2 gene, Per2.Biomolecules & Therapeutics, 26(4), 358–367.
34. Kim et al. (2021) Multiplexed CRISPR-Cas9 system in a single adeno-associated virus to simultaneously knock out redundant clock genes.
35. Korshunov, K. S., Blakemore, L. J. & Trombley, P. (2017). Dopamine: a modulator of circadian rhythms in the central nervous system. Frontiers in Cellular Neuroscience, 11, article number: 91.
36. Landgraf D., Wang, L., Diemer T., Welssh DK., (2016) NPAS2 Compensates for Loss of CLOCK in Peripheral Circadian Oscillators. PLOS GENETICS. https://doi.org/10.1371/journal.pgen.1005882
37. Lanza A., Timothy J Dyess J., Alper S. (2012) Using the Cre/lox system for targeted integration into the human genome: LoxFAS-loxP pairing and delayed introduction of Cre DNA improve gene swapping efficiency. Biotechnology Journal 7(7):898-908 DOI: 10.1002/biot.201200034. SourcePubMed

38. Laloum., D., Robinson-Rechavi, M. (2020) Methods detecting rhythmic gene expression are biologically relevant only for strong signal. Computational Biology. https://doi.org/10.1371/journal.pcbi.1007666S
39. Levanon, E., (2014): "Human housekeeping genes, revisited." In: Trends in Gen., Mar; 30(3):119-20.
40. Lindberg et al,. (2018). Purinergic Signaling in Neuron-Astrocyte Interactions, Circadian Rhythms, and Alcohol Use Disorder. Front. Physiol., https://doi.org/10.3389/fphys.2018.00009
41. Li CT., Yang KC., Lin WC (2019). Glutamatergic Dysfunction and Glutamatergic Compounds for Major Psychiatric Disorders: Evidence From Clinical Neuroimaging Studies. Front. Psychiatry. https://doi.org/10.3389/fpsyt.2018.00767
42. Livak KJ, Schmittgen TD. (2001) Analysis of Relative Gene Expression Data Using RealTime Quantitative PCR −2ΔΔCt Method. 25:402–8.
43. Lucena-Aguilar G., Sanchez-Lopez A-M, Barberan-Aceteuno C., Carrilo-Avila JA., Lopez-Guerrera JA., Aguilar-Quesada R., (2016) DNA Source Selection for Downstream Applications Based on DNA Quality Indicators Analysis. Biopreservation and Biobanking. doi: 10.1089/bio.2015.0064
44. Marchand, W. R. & Yurgelunn-Todd, D. (2010). Striatal structure and function in mood disorders: a comprehensive review. Bipolar Disorders, 12(2010), 764–785. doi:10.1111/j.1399-5618.2010.00874.x
45. McClung, C. (2013). How might circadian rhythms control mood? Let me count the ways.Biological Psychiatry, 74(4), 242–249. G
46. McClung C. (2019). Rhythms of life: circadian disruption and brain disorders across the lifespan. Nat Rev Neurosci. 2019 Jan; 20(1): 49–65.doi: 10.1038/s41583-018-0088-y accessed at: https://www.frontiersin.org/articles/10.3389/fneur.2020.00398/full
47. Mendoza, J. & Challet, E. (2014). Circadian insights into dopamine mechanisms. Neuroscience, 282, 230–242. doi:10.1016/j.neuroscience.2014.07.081
48. Medline Plus (2020). A2a gene. Accessed at: https://medlineplus.gov/genetics/gene/a2a
49. Medline Plus (2020). Maoa gene. Accessed at: https://medlineplus.gov/genetics/gene/mao
50. Munoz, E., Brewer, M., Baler, R., (2006) Modulation of Bmal/Clock/E-Box complex activity by a CT-rich cis-acting element. Mol Cell Endocrinology. doi: 10.1016/j.mce.2006.03.007. Epub 2006 May 2
51. Ono, D., Honma K-I., Homno S (2020). GABAergic mechanisms in the suprachiasmatic nucleus that influence circadian rhythm. Journal of Neurochemistry. https://doi.org/10.1111/jnc.150124040
52. Ono, D., Honma K-I., Yanagawa Y., Yamanaka A. (2018) Role of GABA in the regulation of the central circadian clock of the suprachiasmatic nucleus. The Journal of Physiological Sciences. DOI:10.1007/s12576-018-0604-x.
53. Ozburn AR., Kern J., Parekh PR. Logan RW. Liu Z., Falcon E., Becker-Krail D., Purohit K., Edgar NM., Huang Y, McClung (2017) NPAS2 Regulation of Anxiety-Like Behavior and GABAA Receptors. https://doi.org/10.3389/fnmol.2017.00360
54. Osbourne, J. W. & Overbay, A. (2004). The Power of Outliers (and Why Researchers Should Always Check for Them). Practical Assessment, Research & Evaluation, 9. http: //PAREonline.net/getvn.asp?v=9&n=6
55. Ozburn et al,. (2015). Direct regulation of diurnal Drd3 expression and cocaine rewardby NPAS2. doi:10.1016/j.biopsych.2014.07.030.
56. Ozburn et al,. (2017) NPAS2 Regulation of Anxiety-Like Behavior and GABAA Receptors. Frontiers in Molecular Neuroscience.
57. Patmanathan et al. - CRISPR/Cas9 in Stem Cell Research: Current Application and Future. Perspective (2018) accessed at: https://www.ncbi.nlm.nih.gov/pubmed/29895256

58. Primer 3. (2012) accessed at: https://bioinfo.ut.ee/primer3-0.4.0/
59. QIAGEN (2013) Frequently Asked Questions. Accessed at: https://www.qiagen.com/ca/resources/faq?id=527bfcc9-9bc3-4990-b439-h61df2f2b06be&lang=en
60. Ripperger, J. A. & Schibler, U. Rhythmic CLOCK-BMAL1 binding to multiple E-box motifs drives circadian Dbp transcription and chromatin transitions. (2006) Nat Genet 38, 369-374, doi:10.1038/ng1738
61. Rey, G., François Cesbron,Jacques Rougemont,Hans Reinke,Michael Brunner,Felix Naef (2011). Genome-Wide and Phase-Specific DNA-Binding Rhythms of BMAL1 Control Circadian Output Functions in Mouse Liver. Plos Biology. https://doi.org/10.1371/journal.pbio.1000595
62. Sánchez, V. (1995). Circadian variations of adenosine and of its metabolism. Could adenosine be a molecular oscillator for circadian rhythms? Can. J. Physiol. Pharmacol. 73, 339–355. doi: 10.1139/y95-044
63. Schnell., A., Federica Sandrelli,Vaclav Ranc,Jürgen A. Ripperger,Emanuele Brai,Lavinia Alberi (2015)., Mice lacking circadian clock components display different mood-related behaviors and do not respond uniformly to chronic lithium treatment.
64. Schoettner., K., Alonso., M, Button M, Cassandra G, Herrera J, Quteishat N, Meyer C, Bergdahl A & Amir, S. (2022). Characterization of Affective Behaviors and Motor Functions in Mice With a Striatal-Specific Deletion of Bmal1 and Per2. Front. Physiol., Sec. Chronobiology
65. Takahashi, J. S. (2017). Transcriptional Architecture of the Mammalian Circadian Clock. Nat. Rev. Genet. 18, 164–179. doi:10.1038/nrg.2016.150
66. ThermoFischerScientific (2022)Assessing RNA quality. Accessed at: https://www.thermofisher.com/ca/en/home/references/ambion-tech-support/rna-isolation/tech-notes/assessing-rna-quality.html
67. Usiello et al., (2000). Distinct functions of the two isoforms of dopamine D2 receptors. Nature volume 408, pages199–203
68. Varinthra, P., Liu., X., (2019). Molecular basis for the association between depression and circadian rhythm. Apr-Jun; 31(2): 67–72.doi: 10.4103/tcmj.tcmj_181_18
69. Vetter. C., (2018). Circadian disruption: What do we actually mean? https://doi.org/10.1111/ejn.14255
70. Williams, OF., Coppolino, M., George RS., Perrault ML. (2021). Sex Differences in Dopamine Receptors and Relevance to Neuropsychiatric Disorders. 11(9), 1199; https://doi.org/10.3390/brainsci11091199

Appendix A: Summary Statistics and Analysis of Variance Source Table (*GABRR1*)

Table A1

Means and standard deviations of relative expression of Gabbra1 in males, 2x2 factorial design

Genotype	Time Point	M	SD	N
WT	**ZT2**	**1.384**	**0.266**	**3**
	ZT14	0.476	0.837	3
KO	ZT2	0.632	0.02	3
	ZT14	0.625	-	1
Total	ZT2	1.008	0.532	6
	ZT14	0.5505	0.105	4

Note. M & SD represent the mean and standard deviation of each genotype at each time point, respectively.

Table A2

Means and standard deviations of relative expression of Gabbra1 in females, 2x2 factorial design

Genotype	Time Point	M	SD	N
WT	**ZT2**	***1.006***	**0.133**	**3**
	ZT14	*0.919*	0.206	3
KO	ZT2	*0.758*	0.225	3
	ZT14	*0.749*	0.195	3
Total	ZT2	0.882	0.175	6
	ZT14	0.834	0.120	6

Note. M & SD represent the mean and standard deviation of each genotype at each time point, respectively.

Table A3

Analysis of Variance Results for relative expression, Males

Source	SS	DF	MS	F	P
Genotype	**0.1067**	**1**	**0.1067**	**0.4146**	**.54**
Time Point	0.0638	1	0.0638	0.2479	.64
Genotype*Time Point	0.0019	1	0.0019	0.0074	.93
Error	1.544	6	0.2573		

Note. WT (n = 6) & KO (n = 4)

Table A4

Analysis of Variance Results for relative expression, Females

Source	SS	DF	MS	F	P
Genotype	**0.1311**	**1**	**0.1311**	**3.521**	**.10**
Time Point	0.0069	1	0.0069	0.1853	.68
Genotype*Time Point	0.0044	1	0.0044	0.1190	.74
Error	0.2978	8	0.03723		

Note. WT (n = 6) & KO (n = 6)

Appendix B: Summary Statistics and Analysis of Variance Source Table (*GAD67*)

Table B1

Means and standard deviations of relative expression of GAD67 in males, 2x2 factorial design

Genotype	Time Point	M	SD	N
WT	**ZT2**	**1.024**	**0.271**	**3**
	ZT14	2.256	1.297	3
KO	ZT2	0.753	0.262	3
	ZT14	0.914	-	1
Total	ZT2	0.889	0.191	6
	ZT14	1.585	0.949	4

Note. M & SD represent the mean and standard deviation of each genotype at each time point, respectively.

Table B2

Means and standard deviations of relative expression of GAD67 in females, 2x2 factorial design

Genotype	Time Point	M	SD	N
WT	**ZT2**	**1.002**	**0.074**	**3**
	ZT14	0.956	0.330	3
KO	ZT2	1.077	0.747	3
	ZT14	1.236	0.336	3
Total	ZT2	1.039	0.053	6
	ZT14	1.096	0.198	6

Note. M & SD represent the mean and standard deviation of each genotype at each time point, respectively.

Table B3

Analysis of Variance Results for relative expression, Males

Source	SS	DF	MS	F	P
Genotype	**1.301**	**1**	**1.301**	**2.138**	**.19**
Time Point	0.9704	1	0.970	1.595	.25
Genotype*Time Point	0.5731	1	0.573	0.9421	.37
Error	3.650	6	0.6084		

Note. WT (n = 6) & KO (n = 4)

Table B4

Analysis of Variance Results for relative expression, Females

Source	SS	DF	MS	F	P
Genotype	**0.0950**	**1**	**0.0950**	**0.4841**	**.51**
Time Point	0.0009	1	0.0009	0.04882	.83
Genotype*Time Point	0.0316	1	0.03156	0.1608	.70
Error	1.570	8	0.1963		

Note. WT (n = 6) & KO (n = 6)

Appendix C: Summary Statistics and Analysis of Variance Source Table (*A2a*)

Table C1

Means and standard deviations of relative expression of A2a in males, 2x2 factorial design

Genotype	Time Point	M	SD	N
WT	**ZT2**	**1.097**	**0.606**	**3**
	ZT14	0.822	0.786	3
KO	ZT2	0.881	0.341	3
	ZT14	1.434	-	1
Total	ZT2	0.989	0.153	6
	ZT14	1.128	0.433	4

Note. M & SD represent the mean and standard deviation of each genotype at each time point, respectively.

Table C2

Means and standard deviations of relative expression of A2a in females, 2x2 factorial design

Genotype	Time Point	M	SD	N
WT	**ZT2**	**1.384**	**1.128**	**3**
	ZT14	0.476	0.285	3
KO	ZT2	0.633	0.332	3
	ZT14	1.625	0.193	3
Total	ZT2	1.009	0.531	6
	ZT14	1.051	0.812	6

Note. M & SD represent the mean and standard deviation of each genotype at each time point, respectively.

Table C3

Analysis of Variance Results for relative expression, Males

Source	SS	DF	MS	F	P
Genotype	**0.07837**	**1**	**0.07837**	**0.2136**	**.66**
Time Point	0.03894	1	0.03894	0.1061	.76
Genotype*Time Point	0.3420	1	0.3420	0.9321	.37
Error	2.201	6	0.3669		

Note. WT (n = 6) & KO (n = 4)

Table C4

Analysis of Variance Results for relative expression, Females

Source	SS	DF	MS	F	P
Genotype	**0.2725**	**1**	**0.2725**	**0.7254**	**.42**
Time Point	0.6293	1	0.6293	1.675	.23
Genotype*Time Point	0.6074	1	0.6074	1.617	.24
Error	3.006	8	0.3757		

Note. WT (n = 6) & KO (n = 6)

Appendix D: Summary Statistics and Analysis of Variance Source Table (*DRD2*)

Table D1

Means and standard deviations of relative expression of DRD2 in males, 2x2 factorial design

Genotype	Time Point	M	SD	N
WT	**ZT2**	**1.017**	**0.219**	**3**
	ZT14	1.297	0.817	3
KO	ZT2	1.303	0.645	3
	ZT14	1.386	-	1
Total	ZT2	1.162	0.202	6
	ZT14	1.341	0.063	4

Note. M & *SD* represent the mean and standard deviation of each genotype at each time point, respectively.

Table D2

Means and standard deviations of relative expression of DRD2 in females, 2x2 factorial design

Genotype	Time Point	M	SD	N
WT	**ZT2**	**1.153**	**0.792**	**3**
	ZT14	2.452	0.927	3
KO	ZT2	2.677	1.597	3
	ZT14	2.370	0.830	3
Total	ZT2	1.915	1.078	6
	ZT14	2.411	0.058	6

Note. M & *SD* represent the mean and standard deviation of each genotype at each time point, respectively.

Table D3

Analysis of Variance Results for relative expression, Males

Source	SS	DF	MS	F	P
Genotype	**0.07053**	**1**	**0.07053**	**0.1870**	**.68**
Time Point	0.06582	1	0.06582	0.1745	.69
Genotype*Time Point	0.01926	1	0.01926	0.05108	.83
Error	2.263	6	0.3772		

Note. WT (n = 6) & KO (n = 4)

Table D4

Analysis of Variance Results for relative expression, Females

Source	SS	DF	MS	F	P
Genotype	**1.561**	**1**	**1.561**	**1.321**	**.28**
Time Point	0.7372	1	0.7372	0.6238	.45
Genotype*Time Point	1.934	1	1.934	1.636	.24
Error	9.454	8	1.182		

Note. WT (n = 6) & KO (n = 6)

Appendix E: Summary Statistics and Analysis of Variance Source Table (*MAOA*)

Table E1

Means and standard deviations of relative expression of Maoa in males, 2x2 factorial design

Genotype	Time Point	M	SD	N
WT	**ZT2**	**1.017**	**0.214**	**3**
	ZT14	1.271	0.843	3
KO	ZT2	0.952	0.044	3
	ZT14	1.293	-	1
Total	ZT2	0.985	0.046	6
	ZT14	1.282	0.016	4

Note. M & SD represent the mean and standard deviation of each genotype at each time point, respectively.

Table E2

Means and standard deviations of relative expression of Maoa in females, 2x2 factorial design

Genotype	Time Point	M	SD	N
WT	**ZT2**	**1.001**	**0.074**	**3**
	ZT14	1.010	0.330	3
KO	ZT2	1.020	0.747	3
	ZT14	0.949	0.336	3
Total	ZT2	1.010	0.013	6
	ZT14	0.979	0.043	6

Note. M & SD represent the mean and standard deviation of each genotype at each time point, respectively.

Table E3

Analysis of Variance Results for relative expression, Males

Source	SS	DF	MS	F	P
Genotype	**0.0009**	**1**	**0.0009**	**0.0036**	**.95**
Time Point	0.1771	1	0.1771	0.7002	.43
Genotype*Time Point	0.0037	1	0.0037	0.01145	.91
Error	1.518	6	0.2530		

Note. WT (n = 6) & KO (n = 4)

Table E4

Analysis of Variance Results for relative expression, Females

Source	SS	DF	MS	F	P
Genotype	**1.561**	**1**	**1.561**	**1.321**	**.28**
Time Point	0.7372	1	0.7372	0.6238	.45
Genotype*Time Point	1.934	1	1.934	1.636	.24
Error	9.454	8	1.182		

Note. WT (n = 6) & KO (n = 6)

Appendix F:

Table F: cDNA Synthesis Specifications & Tips

	For cDNA derived from high copy number genes and/or abundant starting material such that RT reactions are performed from 1ug of total RNA perform a 1:10 serial dilution of your cDNA from neat to 1:10,000 dilution
2.	Select an amount of cDNA that yields a Ct value of between 15 to 25 cycles although 10 to 35 is also appropriate providing the triplicates at each dilution are within 0.5 cycles and thus the R2 value in that part of the standard curve is > 0.98.
3.	By implication never take a dilution of cDNA where triplicates begin to diverge and correlation breakdown. In this scenario I would typically end up using about a 1:100 dilution of my cDNA
4.	Nevertheless, select a dilution of cDNA that is at the lower limit of this Ct window where triplicates are still concordant rather than a dilution of cDNA that also yields concordant data and falls within this ambient CT window. This is because at higher Ct concentrations you can potentially increase background and in particular formation of primer dimers
5.	For low copy number genes or where starting material is limited such that you are obliged to reverse transcribe from as little as 100ng of total RNA. Set up a standard curve by performing a 1:2 serial dilution from neat to 1:64 to 1:128. Then follow the above guidance. In these scenarios I typically end up using a 1:16 to 1:32 dilution of my cDNA for gene expression analysis

Appendix G: cDNA Synthesis Specifications & Tips

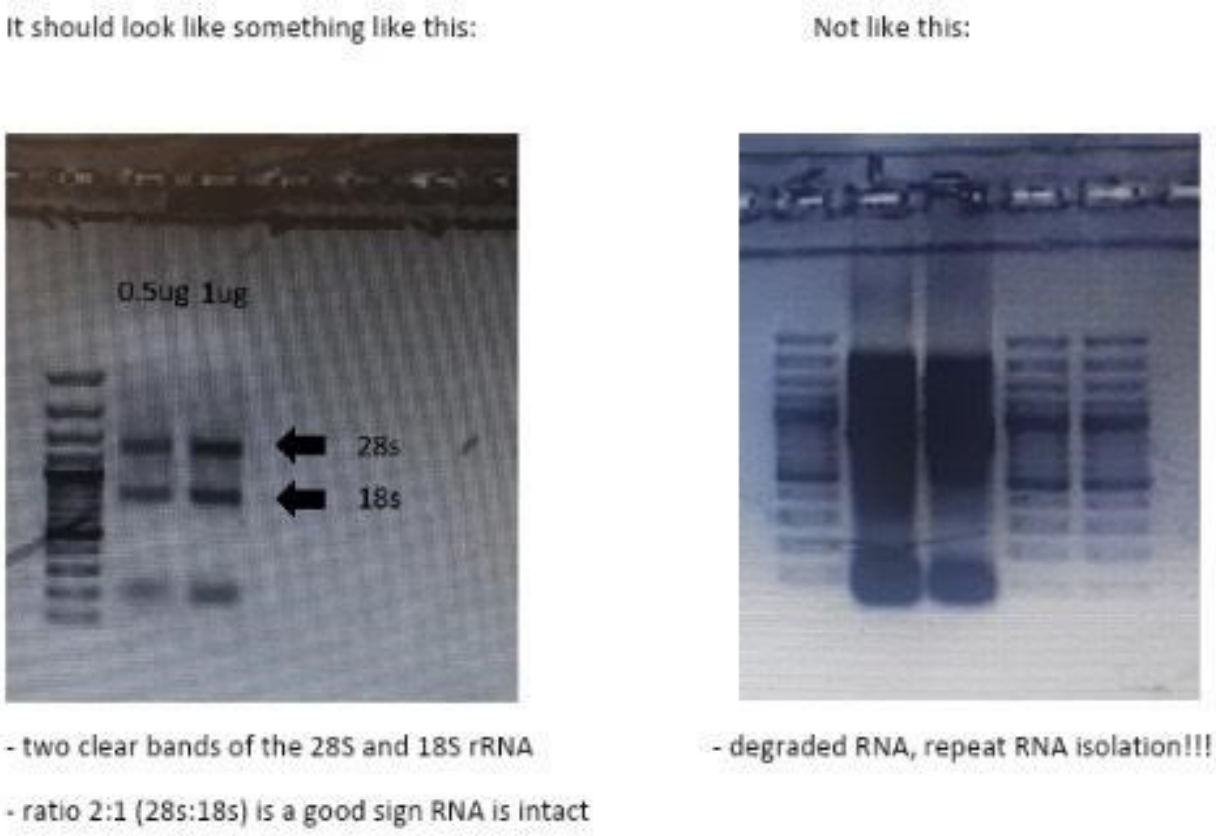

Figure 7. Intact vs. Degraded RNA. Degraded total RNA and intact total RNA were ran along with RNA Markers on a 1% denaturing agarose gel. While the 18S and 18S rRNA bands are clearly visible in the intact RNA sample, there are visible smears that appear at a lower molecular weight in the degraded RNA.